Table 3. ROI values of four groups

ROI	CDR 0 NORMAL (n = 14)	CDR 0.5/NON-CONVERTERS (n = 22)	CDR 0.5/ CONVERTERS (n = 20)	CDR 1+AD (N = 12)	MS	F-VALUE	p-VALUE
Upper frontal	8.58 (1.17)	8.31 (0.43)	8.13 (0.38)	5.73 (0.86)[abc]	22.433	44.054	<0.001
Anterior frontal	7.64 (1.33)	7.09 (0.49)	6.90 (0.63)	4.64 (1.03)[abc]	22.522	30.436	<0.001
Inferior frontal	6.72 (1.31)	6.24 (0.51)	6.08 (0.42)	4.96 (0.90)[abc]	7.061	11.258	<0.001
Parietal	8.35 (1.13)	8.02 (0.42)	7.99 (0.47)	5.46 (0.83)[abc]	23.181	46.317	<0.001
TPO	7.31 (1.13)	6.87 (0.36)	5.84 (0.43)[ab]	4.34 (1.07)[abc]	23.774	43.005	<0.001
Primary auditory	8.81 (0.85)	8.59 (0.44)	8.54 (0.44)	5.16 (0.96)[abc]	39.814	93.525	<0.001
Temporal	6.89 (1.35)	6.42 (0.48)	6.26 (0.53)	4.50 (0.93)[abc]	14.053	20.761	<0.001
Hippocampus	6.20 (0.86)	6.05 (0.52)	5.45 (0.70)[a]	4.50 (0.95)[abc]	8.106	15.092	<0.001
Primary visual	9.34 (1.24)	8.43 (0.51)	8.19 (0.63)	5.70 (0.84)[abc]	29.721	24.293	<0.001
Occipital	7.91 (1.18)	7.11 (0.50)	6.54 (0.91)	4.16 (0.82)[abc]	42.626	52.311	<0.001
Basal ganglia	6.58 (1.16)	6.43 (0.27)	6.38 (0.30)	6.02 (0.76)	0.723	1.716	0.172
Cerebellum	7.32 (1.20)	7.39 (0.31)	7.27 (0.43)	6.06 (1.00)[abc]	5.371	9.721	<0.001
White matter	5.94 (1.08)	5.70 (0.32)	5.62 (0.52)	5.38 (0.88)	0.701	1.458	0.234

Shown are the means (SD).
The AD group had severely decreased rCMRglc compared with other groups, except in the basal ganglia and white matter (multiple ANOVAs and post hoc tests). There were no significant differences between CDR 0.5/non-converters and the CDR 0 group. However, CDR 0.5/Converters had decreased rCMRglc in the TPO and hippocampus compared with CDR 0 subjects, and decreased rCMRglc in the TPO compared with CDR 0.5/non-converters.
post hoc tests, significantly ($p<0.05$) different from Normal (a), CDR 0.5/non-converters (b), and CDR 0.5/converters (c).
ROI = region of interests, TPO = Temporo-parieto-occipital, CDR = Clinical Dementia Rating, con. = converters, AD = Alzheimer's disease.

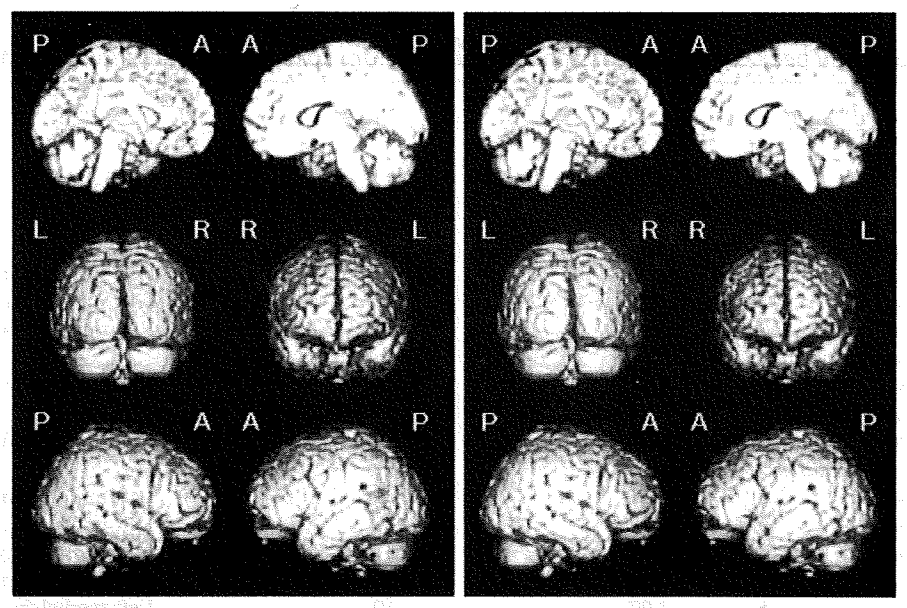

(a) CDR 0.5/Converters < CDR 0 (b) CDR 0.5/Non-converters < CDR 0

Figure 1. Results from voxel-based analysis with SPM2. (a) Voxels showing significant hypometabolism for CDR 0.5/converters compared to CDR 0 subjects ($p<0.001$, uncorrected). (b) Voxels showing significant hypometabolism for CDR 0.5/non-converters compared to CDR 0 subjects ($p<0.001$, uncorrected). The local maxima for the brain regions are shown in Table 3.

patients are shown in Figure 2. A region of hypometabolism was considered significant at $p<0.001$ (uncorrected) for a cluster of ≥ 20 contiguous voxels superimposed on 3D-rendered MR images in Montreal Neurological Institute (MNI) space (Evans *et al.*, 1994). Brain areas reaching the significance threshold were identified by voxel coordinates and labeled according to Talairach and Trournoux after coordinate conversion from MNI to Talairach space using a non-linear transformation algorithm (http://imaging.mrc-cbu.cam.ac.uk/imaging/MniTalairach) (Talairach and Trournoux,

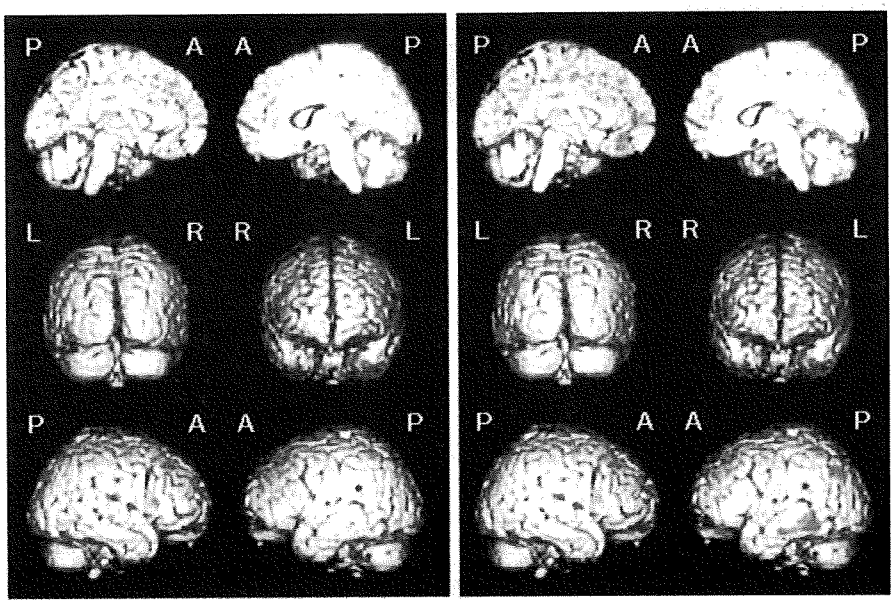

(a) AD < CDR 0.5/Converters (b) AD < CDR 0.5/Non-converters

Figure 2. (a) Voxels showing significant hypometabolism for patients with AD compared to CDR 0.5/converters ($p<0.001$, uncorrected). (b) Voxels showing significant hypometabolism for patients with AD compared to CDR 0.5/non-converters ($p<0.001$, uncorrected).

Table 4. Location and peak coordinates of significant voxels from voxel-based analysis using SMP2

TALAIRACH COORDINATES			T STATISTICS	BRODMANN	ANATOMIC REGION
x	y	z			
CDR 0.5/converters < CDR 0					
−44	−53	19	4.04	22	Left superior temporal gyrus
−44	−46	17	3.57	22	Left superior temporal gyrus
36	−36	−13	4.01	36	Right parahippocampal gyrus
CDR 0.5/con-converters < CDR 0					
8	51	20	3.59	9	Right medial frontal gyrus
AD < CDR 0.5/converters					
44	20	10	4.04	45	Right inferior frontal gyrus
AD < CDR 0.5/non-converters					
−55	−45	−8	4.91	21	Left middle temporal gyrus
−57	−32	−15	3.77	20	Left inferior Temporal gyrus
−26	−45	−8	4.14	37	Left fusiform gyrus
46	18	10	4.08	45	Right inferior frontal gyrus
−10	57	5	3.97	10	Left medial frontal gyrus
−12	38	−20	3.70	11	Left straight gyrus
−5	34	−8	3.54	32	Left cingulate gyrus
−44	−71	35	3.37	39	Left angular gyrus
CDR 0.5/converters < CDR 0.5/non-converters					
−40	−61	25	3.85	39	Left middle temporal gyrus
−46	−40	22	3.61	40	Left inferior parietal lobule
12	−37	37	3.61	31	Right cingulate gyrus
−55	−43	−11	3.51	37	Left inferior temporal gyrus

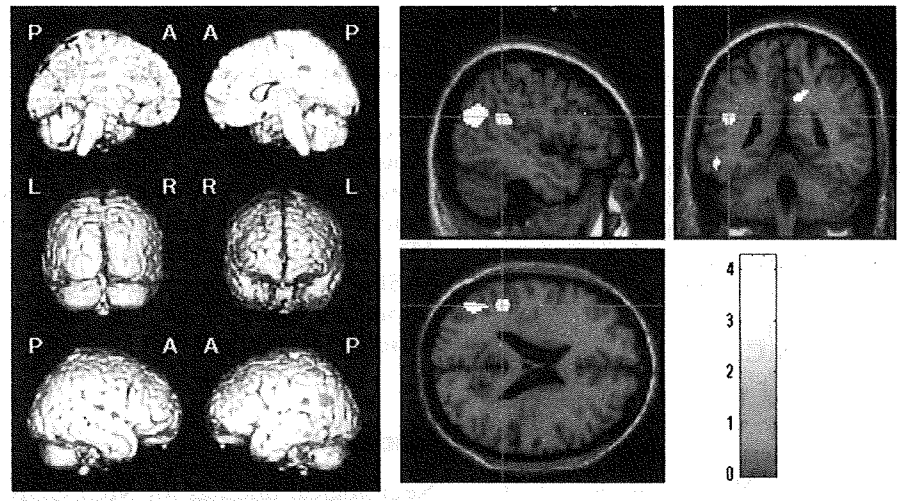

CDR 0.5/Converters < CDR 0.5/Non-converters

Figure 3. (Left) Voxels showing significant hypometabolism for CDR 0.5/converters compared to CDR 0.5/non-converters ($p<0.001$, uncorrected). (Right) The same results were displayed on 2D planes of a normal MRI template provided by SPM2 to clarify their anatomic locations. The color bar represents t values derived from the voxel-based analysis.

Table 5. PET patterns of Silverman's classification for two CDR 0.5 groups

	N1	N2	N3	P1	P2	P3	TOTAL
Non-converters	5	5	7	5	0	0	23
Converters	3	1	4	12	0	0	20

N = non-progressive patterns, p = progressive patterns

1998). Areas showing a significant difference (SPM2, $p<0.001$, uncorrected) are shown in Table 4. For multiple comparisons, the significance level was set at 0.001.

Comparison between CDR 0.5/converters and CDR 0.5/non-converters

CDR 0.5/converters had significantly lower CMRglc values (SPM2, $p<0.001$, uncorrected) in the left middle temporal gyrus, left inferior parietal lobule, right cingulate gyrus, and left inferior temporal gyrus, compared with CDR 0.5/non-converters (Figure 3 and see Table 4).

Individual analysis using Silverman's classification

PET patterns using Silverman's classification for the two CDR 0.5 groups are shown in Table 5. The difference between the groups was significant by χ^2 test ($p<0.05$), with CDR 0.5/converters showing a P1 pattern more frequently. No participants showed P2 or P3 patterns. Comparing all non-progressive patterns (N1–N3) with the progressive pattern (P1) for the two groups, a true positive rate (sensitivity) of 0.60, a true negative rate (specificity) of 0.74, a positive predictive value of 0.71, and a negative predictive value of 0.68 were found. Of the 14 normal subjects, 12 showed an N1 pattern and 2 had an N2 pattern. The 12 AD patients all showed P1 patterns.

Discussion

In this study, CDR 0.5/converters showed greater baseline hypometabolism compared with CDR 0.5/non-converters in brain areas specific for AD, suggesting that CDR 0.5 converters might have AD-like changes.

Methodological issues

There are some methodological limitations in the study. First, only 40% of the CDR 0 subjects and 70% of the CDR 0.5 subjects were scanned due to limited availability of the FDG-PET scanner (an average of four patients a month). The long distance between Tajiri and the PET center also prevented some older adults from participating in the study. Therefore, there may be some sampling bias and caution is required in interpretation of the results. Second, evaluation was only performed at two time points, rather than annually; however, the administrative situation brought about by the formation of a new city in 2006 through the merger of several towns, including Tajiri, prevented use of an annual study design. Third, although the CASI provided sufficient information for a detailed analysis, assessments such as the WMS-R for memory and the WAIS-R for general intelligence would have provided more cognitive information; however, the time required for assessing community residents prevented use of these tests.

Neuropsychological findings

Only the CASI "recent memory" score showed a significant difference between CDR 0.5/converters and CDR 0.5/non-converters ($p = 0.008$). This is consistent with previous studies (Arnaiz *et al.*, 2001; Visser *et al.*, 2002) and suggests that CDR 0.5/converters already have AD-like changes, since recent memory impairment is a well-known neuropsychological feature of AD.

Criteria for amnestic MCI

We evaluated the effect of amnestic MCI criteria retrospectively. Among the CDR 0.5 group, those who met the following criteria were also considered to have amnestic MCI (Meguro *et al.*, 2004): memory complaints, a CASI "recent memory" score of −1.5 SD lower than the normal values for each age group, and normal MMSE scores for each educational level. Four CDR 0.5 subjects met these criteria and all converted to AD. Although the sample size was small, these results suggest that criteria for amnestic MCI are more "specific" for AD changes, whereas CDR 0.5 criteria are more "sensitive."

Metabolic patterns of CDR 0.5 converters

The lack of metabolic differences after taking CASI scores into covariance might indicate that cognitive, rather than metabolic, differences predict conversion to AD. However, the aim of this study was to investigate whether metabolic changes in CDR 0.5 converters manifest as a decrease in CMRglc in a manner specific to early AD. Although the predictive power may be stronger for cognitive dysfunction, we believe that the findings support the hypothesis of the study.

Our findings suggest that CDR 0.5 participants who decline to AD develop hypometabolism in the posterior cingulate and other brain regions that might be specific to AD. These hypometabolic areas are similar to those observed in patients with probable AD (Hoffman *et al.*, 2000). Previous longitudinal studies on amnestic MCI have also indicated that these areas differ significantly between converters and non-converters (Arnaiz *et al.*, 2001; Chetelat *et al.*, 2003; Drzezga *et al.*, 2003; Mosconi *et al.*, 2004). A follow-up SPECT study on amnestic MCI also showed asymmetric reduction of perfusion in the parahippocampus, lateral parietal lobe, and posterior cingulate cortices in converters (Ishiwata *et al.*, 2006). Parahippocampal gyri are very small areas and other studies may have missed these regions using the SPM method.

Since SPM reveals much more restricted abnormalities than suggested by individual classification, analysis of the individual patterns is required to provide support for SPM findings. In individual analysis of the CMRglc pattern, the AD pattern (P1) was most frequent among CDR 0.5/converters, whereas N1 and N3 patterns were frequent in CDR 0.5/non-converters (Table 5). These results are consistent with past studies and indicate that most CDR 0.5/converters already have AD pathology. The data also support the results of SPM analysis, indicating that both visual and automated methods are preferable to confirm the reliability of acquired data.

Conclusion

Neurological findings for MCI/CDR 0.5 decliners may show manifestation of hypometabolism in brain areas specific to AD. Since the prevalence of CDR 0.5 is much higher than that of MCI and the rate of decline to dementia from the two conditions is about the same, use of CDR 0.5 criteria may increase the detection rate of decliners in a community population.

Conflict of interest

None.

Description of authors' roles

K. Meguro and H. Ishii designed the study, supervised the data collection and wrote the paper. K. Meguro and S. Yamaguchi collected the data. H. Ishikawa and M. Tashiro were responsible for the statistical design of the study and for statistical analysis.

Acknowledgments

We are grateful to the town officials of Tajiri. This study was supported in part by a JST grant for research and education in molecular imaging.

References

American Psychiatric Association (1994). *Diagnostic and Statistical Manual of Mental Disorders*, 4th edn. Washington, DC: American Psychiatric Association.

Arnaiz, E. *et al.* (2001). Impaired cerebral glucose metabolism and cognitive functioning predict deterioration in mild cognitive impairment. *NeuroReport*, 12, 851–855.

Chen, P., Ratcliff, G., Belle, S. H., Cauley, J. A., DeKosky, S. T., and Ganguli, M. (2000). Cognitive tests that best discriminate between presymptomatic AD and

those who remain nondemented. *Neurology*, 55, 1847–1853.

Chetelat, G., Desgranges, B., de la Sayette, V., Viader, F., Eustache, F. and Baron, J. C. (2003). Mild cognitive impairment: can FDG-PET predict who is to rapidly convert to Alzheimer's disease? *Neurology*, 60, 1374–1377.

Drzezga, A. *et al.* (2003). Cerebral metabolic changes accompanying conversion of mild cognitive impairment into Alzheimer's disease: a PET follow-up study. *European Journal of Nuclear Medicine and Molecular Imaging*, 30, 1104–1113.

Evans, A. D. *et al.* (1994). 3D statistical neuroanatomical models from 305 MRI volumes. *IEEE Nuclear Science Symposium Medical Imaging Conference*, 3, 1813–1817.

Fellgiebel, A., Scheurich, A., Bartenstein, P. and Muller, M. J. (2007). FDG-PET and CSF phospho-tau for prediction of cognitive decline in mild cognitive impairment. *Psychiatry Research*, 155, 167–171.

Folstein, M. F., Folstein, S. E. and McHugh, P. R. (1975). "Mini-mental state": a practical method for grading the cognitive state of patients for the clinician. *Journal of Psychiatric Research*, 12, 189–198.

Hoffman, J. M. *et al.* (2000). FDG PET imaging in patients with pathologically verified dementia. *Journal of Nuclear Medicine*, 41, 1920–1928.

Ishiwata, A., Sakayori, O., Minoshima, S., Mizumura, S., Kitamura, S. and Katayama, Y. (2006). Preclinical evidence of Alzheimer changes in progressive mild cognitive impairment: a qualitative and quantitative SPECT study. *Acta Neurologica Scandinavica*, 114, 91–96.

Larrieu, S. *et al.* (2002). Incidence and outcome of mild cognitive impairment in a population-based prospective cohort. *Neurology*, 59, 1594–1599.

McKhann, G., Drachman, D., Folstein, M., Katzman, R., Price, D. and Stadlan, E. M. (1984). Clinical diagnosis of AD: report of the NINCDS-ADRDA work group under the auspices of department of health and human services task force on AD. *Neurology*, 34, 939–944.

Meguro, K. (2004). *A Clinical Approach to Dementia: An Instruction of CDR Worksheet.* Tokyo: Igaku-Shoin.

Meguro, K. *et al.* (2002). Prevalence of dementia and dementing diseases in Japan: the Tajiri Project. *Archives of Neurology*, 59, 1109–1114.

Meguro, K. *et al.* (2004). Prevalence and cognitive performances of Clinical Dementia Rating 0.5 and mild cognitive impairment in Japan: the Tajiri Project. *Alzheimer Disease and Associate Disorders*, 18, 3–10.

Meguro, K. *et al.* (2007) Incidence of dementia and associated risk factors in Japan: The Osaki-Tajiri Project. *Journal of Neurological Sciences*, 260, 175–182.

Morris, J. C. (1993). The Clinical Dementia Rating (CDR): current version and scoring rules. *Neurology*, 43, 2412–2414.

Morris, J. C. *et al.* (2001). Mild cognitive impairment represents early-stage Alzheimer's disease. *Archives of Neurology*, 58, 397–405.

Mosconi, L. *et al.* (2004). MCI conversion to dementia and the APOE genotype: a prediction study with FDG-PET. *Neurology*, 63, 2332–2340.

Perneczky, R., Hartmann, J., Grimmer, T., Drzezga, A. and Kurz, A. (2007). Cerebral metabolic correlates of the Clinical Dementia Rating scale in mild cognitive impairment. *Journal of Geriatric Psychiatry and Neurology*, 20, 84–88.

Petersen, R. C., Smith, G. E., Waring, S. C., Ivnik, R. J., Kokmen, E. and Tangelos, E. G. (1997). Aging, memory, and mild cognitive impairment. *International Psychogeriatrics*, 9, 65–69.

Phelps, M. E., Huang, S. C., Hoffman, E. J., Selin, C., Sokoloff, L. and Kuhl, D. E. (1979). Tomographic measurement of local glucose metabolic rate in humans with (FO-18)2-fluoro-2-deoxy-D-glucose: validation of method. *Annals of Neurology*, 6, 371–388.

Reisberg, B., Ferris, S. H. and de Leon, M. J. (1982). The global deterioration scale for assessment of primary degenerative dementia. *American Journal of Psychiatry*, 139, 1136–1139.

Reivich, M. *et al.* (1979). The ^{18}F-fluoro-deoxyglucose method for the measurement of local cerebral glucose utilization in man. *Circulation Research*, 44, 127–137.

Silverman, D. H. *et al.* (2001). Positron emission tomography in evaluation of dementia: regional brain metabolism and long-term outcome. *JAMA*, 286, 2120–2127.

Talairach, J. and Trournoux, P. (1988). *Co-planar Stereotaxic Atlas of the Human Brain: 3-dimensional Proportional System: An Approach to Cerebral Imaging.* New York: Thieme Medical.

Teng, E. L. *et al.* (1994). The Cognitive Ability Screening Instrument (CASI): a practical test for cross-cultural epidemiological studies of dementia. *International Psychogeriatrics*, 6, 45–58.

Visser, P. J., Verhey, F. R., Hofman, P. A., Scheltens, P. and Jolles, J. (2002). Medial temporal lobe atrophy predicts Alzheimer's disease in patients with minor cognitive impairment. *Journal of Neurology, Neurosurgery, and Psychiatry*, 72, 491–497.

Yamaguchi, S. *et al.* (1997). Decreased cortical glucose metabolism correlated with hippocampal atrophy in Alzheimer's disease as shown by MRI and PET. *Journal of Neurology, Neurosurgery, and Psychiatry*, 62, 596–600.

Altered Brain Serotonin Transporter and Associated Glucose Metabolism in Alzheimer Disease

Yasuomi Ouchi[1,2], Etsuji Yoshikawa[3], Masami Futatsubashi[3], Shunsuke Yagi[1], Takatoshi Ueki[4], and Kazuhiko Nakamura[5]

[1]Molecular Imaging Frontier Research Center, Hamamatsu University School of Medicine, Higashi-ku, Hamamatsu, Japan; [2]Positron Medical Center, Hamamatsu Medical Center, Hamakita-ku, Hamamatsu, Japan; [3]Central Research Laboratory, Hamamatsu Photonics K.K., Hamakita-ku, Hamamatsu, Japan; [4]Department of Neuroanatomy, Hamamatsu University School of Medicine, Higashi-ku, Hamamatsu, Japan; and [5]Department of Psychiatry, Hamamatsu University School of Medicine, Higashi-ku, Hamamatsu, Japan

Whether preclinical depression is one of the pathophysiologic features of Alzheimer disease (AD) has been under debate. In vivo molecular imaging helps clarify this kind of issue. Here, we examined in vivo changes in the brain serotoninergic system and glucose metabolism by scanning early- to moderate-stage AD patients with and without depression using PET with a radiotracer for the serotonin transporter, ^{11}C-3-amino-4-(2-dimethylaminomethylphenylsulfanyl) benzonitrile (DASB), and a metabolic marker, ^{18}F-FDG. **Methods:** Fifteen AD patients (8 nondepressed and 7 depressed) and 10 healthy subjects participated. All participants underwent 3-dimensional MRI and quantitative ^{11}C-DASB PET measurements, followed by ^{18}F-FDG PET scans in the AD group. Region-of-interest analysis was used to examine changes in ^{11}C-DASB binding potential estimated quantitatively by the Logan plot method in the serotonergic projection region. In addition, statistical parametric mapping was used to examine whether glucose metabolism in any brain region correlated with levels of ^{11}C-DASB binding in the dense serotonergic projection region (striatum) in AD. **Results:** Psychologic evaluation showed that general cognitive function (Mini-Mental State Examination) was similar between the 2 AD subgroups. Striatal ^{11}C-DASB binding was significantly lower in AD patients, irrespective of depression, than in healthy controls ($P < 0.05$, corrected), and ^{11}C-DASB binding in other dense projection areas decreased significantly in the depressive group, compared with the control group. The ^{11}C-DASB binding potential levels in the subcortical serotonergic projection region correlated negatively with depression score (Spearman correlation, $P < 0.01$) but not with dementia score. Statistical parametric mapping correlation analysis showed that glucose metabolism in the right dorsolateral prefrontal cortex was positively associated with the level of striatal ^{11}C-DASB binding in AD. **Conclusion:** The significant reduction in ^{11}C-DASB binding in nondepressed AD patients suggests that presynaptic serotonergic function is altered before the development of psychiatric problems such as depression in AD. The depressive AD group showed greater and broader reductions in binding, suggesting that a greater loss of serotonergic function relates to more severe psychiatric symptoms in the disease. This serotonergic dysfunction may affect the activity of the right dorsolateral prefrontal cortex, a higher center of cognition and emotion in AD.

Key Words: Alzheimer's disease; serotonin transporter; glucose metabolism; depression; positron emission tomography

J Nucl Med 2009; 50:1260–1266
DOI: 10.2967/jnumed.109.063008

Alzheimer disease (AD) is a neurodegenerative disorder with progressive memory and cognitive deterioration followed by or concomitant with psychologic problems such as depression and hallucination, which have a strong negative impact on the course of the disease. The occurrence of these psychologic disturbances has been reported to closely relate to disruption of the serotonergic system (*1*). Loss of neurons in the serotonergic raphe nuclei (*2*) and dysfunction of its nerve terminals in the neocortex (*3*) have been reported in AD. Many lines of evidence support this serotonin (5HT) deficiency theory concerning the psychobehavioral symptomatology of AD, as examined in postmortem (*4–6*) and pharmacotherapeutic (*7,8*) studies. A caveat of the postmortem studies is that the findings do not always reflect the antemortem conditions of AD because of variations of clinical symptoms after a mixture of nootropic and psychiatric drugs administered during the patient's lifetime. In addition, the comorbidity of intrinsic depression in patients with AD may be a confounding factor in a study of in vivo serotonergic changes in AD. In vivo studies using PET so far have focused on 5HT receptors in the limbic brain region in association with mnemonic cognitive impairment in AD (*9–11*). Thus, the alterations in presynaptic 5HT function relative to psychologic and behavioral problems in AD with and without depression remain to be investigated.

Received Feb. 9, 2009; revision accepted Apr. 2, 2009.
For correspondence or reprints contact: Yasuomi Ouchi, Laboratory of Human Imaging Research, Molecular Imaging Frontier Research Center, Hamamatsu University School of Medicine, 1-20-1 Handayama, Higashi-ku, Hamamatsu 431-3192, Japan.
E-mail: ouchi@hama-med.ac.jp

The serotonergic projections from the dorsal raphe nucleus are dense in the basal ganglia and thalamus (*12,13*). The 5HT transporter is a component of 5HT presynaptic neurons and a therapeutic target of selective 5HT reuptake inhibitors, which are presently the first-choice treatment for AD patients with depression (*1*). Because the 5HT transporter located on the presynaptic 5HT terminal regulates 5HT signaling, levels of ^{11}C-3-amino-4-(2-dimethylaminomethylphenylsulfanyl) benzonitrile (DASB) binding in these regions reflect the activity of the presynaptic 5HT neurons chiefly in the dorsal raphe nuclei. A recent postmortem study showed a marked reduction in the binding of 5HT transporter tracer in the prefrontal cortex regardless of the presence of depression in AD (*14*). This finding suggests that the loss of raphe nuclei neurons and cortical 5HT transporter is one of the pathologic features of AD at the time of death. In addition, a recent SPECT study on AD with depression showed significantly lower perfusion in the dorsolateral prefrontal cortex (DLPFC) in patients with depressive symptoms than in patients without such symptoms (*15*). The DLPFC is known as a neural substrate of executive function that is consistently compromised in depression (*16*). Furthermore, patients with frontal glucose hypometabolism exhibit a faster deterioration of cognitive abilities (*17*) than do patients with glucose hypometabolism only in the posterior brain. Thus, a combination study of the presynaptic 5HT system and cerebral cortical metabolism is important in elucidating the underlying mechanism for AD with psychotic deterioration.

For this purpose, we measured 2 biomarkers on the same day in mild- to moderate-stage AD patients with and without depression to investigate the levels of presynaptic serotonergic function and cortical neuronal activity using PET with ^{11}C-DASB, a specific 5HT transporter marker, and ^{18}F-FDG.

MATERIALS AND METHODS

Participants

A total of 15 nootropic- and antipsychotic-naïve patients with AD (8 men, 7 women; mean age ± SD, 61.3 ± 5.9 y) and 10 age-, sex-, and education-matched healthy control subjects (5 men, 5 women; mean age, 55.8 ± 8.8 y) participated in the study. The diagnosis of AD was based on the criteria of the National Institute of Neurologic and Communicative Disorders and Stroke and the Alzheimer Disease and Related Disorders Association. The clinical dementia rating in all patients ranged from 1.0 to 1.5, and no patient had psychiatric disorders before the onset of dementia. The participants were evaluated with the Mini-Mental State Examination, the affect test for emotional cognition (subjects evaluate facial expressions on different cards by choosing appropriate answers from the basic emotions: happiness, sadness, surprise, disgust, anger, fear; the full score = 20) (*18*), and the geriatric depression scale (GDS, maximum = 15) for AD patients (*19*). AD patients were classified into 2 subgroups (nondepressed and depressed) according to the GDS scores as shown in Table 1. The present study was approved by the local Ethics Committee of the Hamamatsu University School of Medicine, and written informed consent was obtained from all participants themselves. We obtained written approval from the spouses or family members of AD patients as well.

MRI and PET Procedure

All participants first underwent 3-dimensional MRI just before the PET measurement. We used a static magnet (0.3 T MRP7000AD; Hitachi) with 3-dimensional mode sampling to determine the brain areas for setting the regions of interest (ROIs). The MRI measurements and a mobile PET gantry allowed us to reconstruct PET images parallel to the intercommisural line without reslicing. Using this approach, we were able to allocate ROIs to the target regions of the original PET images (*20*).

PET was performed as described previously (*20*) on a high-resolution brain SHR12000 tomograph (Hamamatsu Photonics K.K.) having an intrinsic resolution of 2.9 × 2.9 × 3.4 mm in full width at half maximum, 47 slices, and a 163-mm axial field of view. After head fixation using a thermoplastic face mask and a 10-min transmission scan for attenuation correction, serial scanning (4 × 30 s, 20 × 60 s, and 14 × 300 s) with periodic arterial blood sampling was performed for 92 min after a slow bolus injection (taking 1 min) of a 300-MBq dose of ^{11}C-DASB with a specific activity of more than 90 GBq/μmol. The method was the same as described previously for another 5HT transporter tracer, ^{11}C-McN5652 (*21*). After completion of the ^{11}C-DASB measurement (after 5 times the half-life of ^{11}C had elapsed), 10 min of emission data were acquired under resting conditions 50 min after

TABLE 1. Clinical Demographics

Category	AD (8 men, 7 women) Nondepressed (4 men, 4 women)	AD (8 men, 7 women) Depressed (4 men, 3 women)	Control (5 men, 5 women)
Age (y)	62.3 (6.4)	60.1 (5.4)	55.8 (8.8)
Education (y)	13.6 (2.2)	14.8 (2.8)	14.0 (2.1)
Disease duration (y)	2.2 (1.5)	1.8 (0.9)	—
Mini-Mental State Examination score	18.9 (3.8)*	17.4 (3.8)*	29.2 (0.8)
Affect test score	12.7 (3.6)*	9.4 (3.7)*†	19.0 (1.1)
GDS score	1.6 (0.8)	8.4 (1.1)*†	0.6 (0.7)

*$P < 0.01$ (paired t test) vs. control.
†$P < 0.01$ vs. nondepressed AD group.
Data are mean values, with SD in parentheses.

injection of 90 MBq of ^{18}F-FDG, according to a previously described autoradiographic technique (*22*).

Image Data Analysis

To determine brain ROIs within the 5HT projection system, we used original morphologic MRI data instead of using spatially normalized MRI data. Most of the cell bodies are in the raphe nuclei in the midsagittal brain stem, with the largest collection of serotonergic neurons residing in the dorsal and median raphe nuclei of the caudal midbrain (*23*). The use of original MR images allowed us to demarcate ROIs on the region covering the substantia nigra (one of the 5HT projection area) on the MR image. In addition, multiple semicircular ROIs (~36–120 mm^2) were drawn bilaterally over the nucleus accumbens, thalamus, putamen, amygdala, prefrontal (Brodmann area 9) and temporal (Brodmann area 21) cortices, and cerebellum on the MR images in reference to an MRI atlas (*24*). These ROIs were then transferred onto the corresponding dynamic ^{11}C-DASB images with 6.8-mm slice-thickness data, generated after adding 2 consecutive slices using image-processing software (Dr View; Asahi Kasei Co.) on a workstation (Ultraspark 300; SUN Microsystems) (*20*).

In the ROI analysis, ^{11}C-DASB binding was quantified using a 2-tissue-compartment model, in which the cerebellar hemisphere was chosen as a reference region. The binding potential (BP) in each target region was calculated by the formula (target tissue Vd)/(cerebellum Vd) − 1, where each Vd (the volume of distribution) was obtained by the Logan graphical method (*25*). Because the pontine and medullary raphe nuclei send a proportion of 5HT axons into the cerebellum, this region is not an ideal candidate for a 5HT-free region. However, the use of the cerebellum as the reference region is acceptable in the present groups because smaller changes in the 5HT system were reported in the cerebellum (*26*).

In voxelwise analysis of ^{18}F-FDG data, all original PET data were converted into semiquantitative parametric images using a unit of standardized uptake denoting the tracer activity per injected dose normalized to body weight. Correlation analysis by statistical parametric mapping (SPM) was performed to examine neural correlates with the level of ^{11}C-DASB binding in the dense 5HT projection area—putamen in the AD group.

Statistics

First, right and left values for the ROIs in each region were averaged because no significant difference was observed between the interhemispheric values with the Student *t* test. Then, the regional ^{11}C-DASB BP values were compared among the 3 groups with 1-way ANOVA using a post hoc Student–Newman–Keuls test. Statistical significance was set at $P < 0.05$ because post hoc multiple comparisons were performed in the analyses. In addition, the Kendall τ test was performed to compare the regional ^{11}C-DASB BP values with the clinical variables in the AD group. The level of significance for the Kendall τ test was set at $P < 0.01$.

For the voxelwise mapping analysis, SPM software was used (SPM2; Wellcome Department of Cognitive Neurology). The standardized uptake value–based ^{18}F-FDG images were then smoothed with an isotropic gaussian kernel of an 8 × 8 × 8 mm filter, as described elsewhere (*27*). Voxel-based correlation between cerebral ^{18}F-FDG uptake and the ^{11}C-DASB BP in the dense 5HT projection area was computed by covariance analysis, using age as a confounding covariate. The statistical threshold was set at $P < 0.001$, and *P* values were left uncorrected.

RESULTS

Levels of ^{11}C-DASB Binding in the 3 Groups

One-way ANOVA showed that the levels of ^{11}C-DASB BP in the dense 5HT projection regions (midbrain, nucleus accumbens, putamen, and thalamus) of the depressed AD group and the level in the putamen of the nondepressed AD group were significantly lower than those in the control group (Table 2; Fig. 1). ^{11}C-DASB BP tended to be reduced in other dense projection areas of the 5HT system (nucleus accumbens, thalamus, and midbrain) in the nondepressed AD group. No significant reduction was found in the cortical areas of the AD group. No significant difference in ^{11}C-DASB binding was found between the nondepressed and depressed AD groups, although the depressed AD group showed a clear tendency toward lower levels. Representative ^{11}C-DASB PET images of subjects in each group are shown in Figure 1.

Correlation Between ^{11}C-DASB Binding and Clinical Parameters in AD Group

As shown in Figure 2A, the levels of ^{11}C-DASB BP in all dense 5HT projection regions correlated negatively with GDS scores (midbrain: $r = 0.692$, $P < 0.01$, $f(x) = -0.057x + 1.834$; putamen: $r = 0.72$, $P < 0.005$, $f(x) = -0.046x + 1.683$; thalamus: $r = 0.839$, $P < 0.005$, $f(x) = -0.046x + 1.638$), indicating that lower binding of ^{11}C-DASB in the 5HT system may be related to greater deterioration of the emotional state in AD. Although no significant correlation was found with the scores for dementia (Mini-Mental State Examination, Fig. 2B) or emotional cognition (affect test, Fig. 2C), there was a tendency toward positive correlations between the putaminal ^{11}C-DASB BP and the Mini-Mental State Examination scores and between subcortical ^{11}C-DASB BPs and the affect scores.

Neural Correlates of Cerebral Glucose Metabolism with Striatal ^{11}C-DASB Binding in AD Group

SPM correlation analysis showed that glucose metabolism in the right DLPFC and superior frontal gyrus corre-

TABLE 2. Levels of ^{11}C-DASB BP in the 3 Groups

	AD		
Brain region	Nondepressed	Depressed	Control
Midbrain	1.73 (0.32)	1.34 (0.15)*	2.01 (0.55)
Nucleus accumbens	1.18 (0.21)	1.03 (0.55)*	1.64 (0.37)
Putamen	1.54 (0.12)*	1.27 (0.25)*	2.05 (0.50)
Thalamus	1.64 (0.18)	1.35 (0.11)*	2.00 (0.23)
Amygdala	1.14 (0.32)	0.80 (0.31)	1.21 (0.34)
Prefrontal cortex	0.28 (0.11)	0.21 (0.08)	0.35 (0.18)
Temporal cortex	0.37 (0.10)	0.29 (0.09)	0.40 (0.11)

*$P < 0.05$ vs. control (Student–Newman–Keuls test).
Data are mean values, with SD in parentheses.

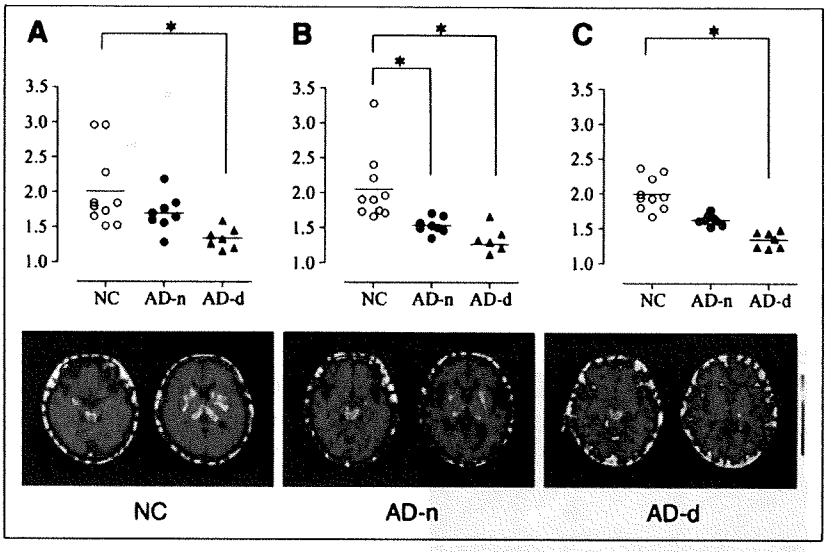

FIGURE 1. Levels of ^{11}C-DASB binding within dense 5HT projection areas in midbrain (A), putamen (B), and thalamus (C). Representative PET images of ^{11}C-DASB binding relative to cerebellar uptake are shown. Color scale denotes magnitude of tissue-to-cerebellum ratio, ranging from 0 to 3. NC = healthy control; AD-n = nondepressive AD; AD-d = depressive AD. *$P < 0.05$, ANOVA with post hoc Student–Newman–Keuls test.

lated positively with putaminal ^{11}C-DASB binding in AD patients (glass brain: Fig. 3A; Table 3). No other significant correlation was found, but there was a tendency toward a correlation when either ^{11}C-DASB BP in the thalamus or BP in the midbrain was chosen as a covariate (data not shown). The glucose metabolic level in the statistically highest peak region (right DLPFC) statistically correlated negatively with GDS scores in AD patients (Fig. 3B, scattergram, $r = 0.798$, $P < 0.0004$, $f(x) = -2.34x + 12.8$). Between-group comparison of SPM failed to show any brain region with statistically significant differences in glucose metabolism between the nondepressed and depressed groups (data not shown).

DISCUSSION

The present results showed a significant reduction in binding of the 5HT transporter marker ^{11}C-DASB in subcortical 5HT projection areas (especially the striatum) in patients with early- to moderate-stage AD regardless of depression and that the reduction was associated with the severity of their depressive states. The brain mapping analysis depicted the right DLPFC as a neural correlate of raphe-striatal 5HT activity in the disease. Furthermore, DLPFC metabolism was found to correlate with depressive scores, suggesting that 5HT dysfunction might affect right DLPFC activity, possibly leading to the generation of a clinical phenotype depression in AD. Thus, as suggested ex vivo (*3,28*), a progressive 5HT dysfunction may be present in the living brain of patients even in the absence of depression and may worsen the state of emotion.

In the present study, ^{11}C-DASB binding in the basal ganglia and thalamus in AD patients was about 25% that in healthy subjects—a smaller reduction than the loss of 5HT cell density observed in the raphe nucleus of postmortem AD brains (45%) (*29*). Although this difference might be due to differences between antemortem and postmortem specimens, a previous finding that marked 5HT cell attrition occurs regardless of the presence or absence of depression (*29*) and our finding that striatal ^{11}C-DASB binding is reduced in parallel with GDS scores suggest that 5HT neuronal reduction and psychologic deterioration may covary up to the last stage of 5HT neuronal loss in AD patients. Indeed, the 5HT neurons may be affected early in the course of the disease because AD patients with GDS scores of around zero showed a marked reduction in ^{11}C-DASB

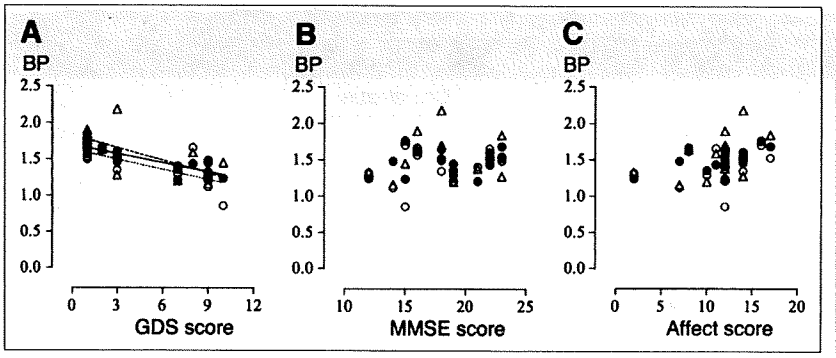

FIGURE 2. Correlations between levels of ^{11}C-DASB BP in midbrain (△), putamen (○), and thalamus (●) for GDS score (A), Mini-Mental State Examination (MMSE) score (B), and affect score (C) in all AD patients. Dotted (putamen), straight (thalamus), and dashed (midbrain) lines denote significant correlations (Kendall rank correlation, $P < 0.01$).

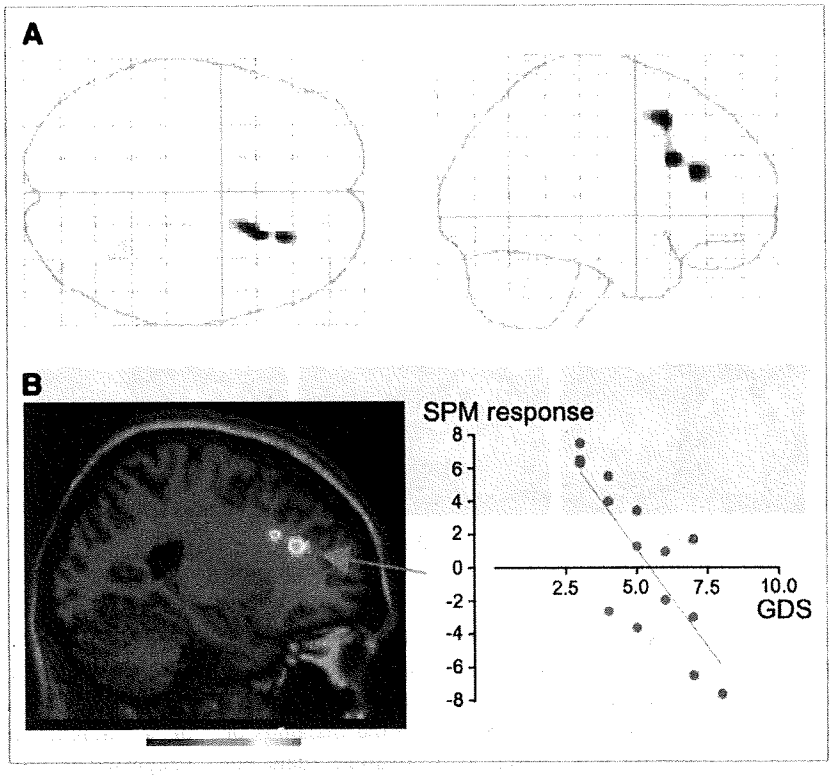

FIGURE 3. SPM images in AD group. (A) SPM correlation analysis showed positive correlation between striatal ^{11}C-DASB BP and glucose use in right DLPFC (glass brain, $P < 0.001$, uncorrected). (B) SPM responses in area with highest peak (arrow) correlated negatively with GDS scores. Color scale bar denotes t value.

binding specifically in the putamen, compared with that in healthy subjects (Fig. 1B). This finding is in contrast to the increase in binding of 5HT transporter marker ^{11}C-McN5652 in major depression, (*30*) suggesting that the underlying etiologies are clearly different. The mechanism of 5HT neuronal degeneration in AD remains unclear, but previous reports about the extent of 5HT neuron loss in the dorsomedial raphe nuclei (*28*) without association between 5HT transporter polymorphism and depression in depressed AD patients (*31*) suggest that the 5HT neuronal degeneration seems acquired. This may be true, because aggregation of Aβ protein exerts an early, focal neurotoxic effect on 5-HT and ACh axons (*32*).

It was reported that glucose metabolism in the DLPFC was lower in depressed AD patients than in their nondepressed counterparts (*33*). In the present study, we found a significant correlation between striatal ^{11}C-DASB binding and DLPFC glucose metabolism (Fig. 3A), the magnitude of which was associated with the extent of clinical deterioration and depression severity. Although striatal ^{11}C-DASB binding was lower in depressed AD patients in the present study, SPM analysis performed separately in each subgroup of AD (nondepressed and depressed) failed to show statistical significance for any brain region (data not shown). This result may be ascribed to the limited number of patients in each group or the narrow variation in ^{11}C-DASB BP in each subgroup. Previous studies showing that the DLPFC was involved in cognitive processing in negative emotion (*34*) and that successful 5HT augmentation therapy activated prefrontal glucose metabolism (*35*) would support our finding that striatal 5HT activity is associated with right DLPFC metabolism in AD patients. This right-

TABLE 3. Brain Regions Showing Significant Correlation Between Glucose Metabolism and Striatal ^{11}C-DASB Binding in AD

Brain region	Brodmann area	Coordinates			z score
		x	y	z	
Positive correlation					
Right DLPFC	9/46	22	22	28	3.91
Right superior frontal gyrus	8	20	16	48	3.79
Negative correlation (none)					

Height threshold, $P < 0.001$ (uncorrected); extent threshold, >100 voxels.

sided dominancy may reflect a depression-related susceptibility because lesions in the right frontal cortex lead to anxiety and depression (*36*) and because recent memories preferentially involve the right prefrontal cortex in AD (*37*). Thus, there might be a link between this important clinical phenomenon and a 5HT-related alteration in right prefrontal activity.

In the present study, no significant correlation was found between presynaptic 5HT dysfunction and dementia, whereas the scattergrams of Figures 2B and 2C showing a weak tendency toward a correlation may hint that a greater number of patients would exhibit significant correlations in presynaptic 5HT activity and these cognitive abilities. In addition, the limited number of clinical features in AD in the current study may be responsible for the failure in clinicobiochemical correlation. Previous reports showing that a reduction in 5HT signaling causes synaptic dysfunction and neuronal death in AD (*38*) and that enhanced 5HT signaling reduces levels of Aβ protein in the brain of transgenic AD mice (*39*) would support this speculation. At the moment, however, it is unlikely that the 5HT system is directly involved in the generation of dementia, as opposed to the implications of cholinergic failure in the AD brain. Because a history of depression is a risk factor of AD, alteration in the 5HT system even at an early stage of the disease should be borne in mind in the management of AD patients. Indeed, in the clinical setting, AD patients with neuropsychiatric symptoms tend to be institutionalized sooner than those without (*40*). Thus, on top of anticholinergic and antiamyloid deposition therapy, enhancement of 5HT signaling by, for example, selective 5HT reuptake inhibitors may be important in the treatment and prophylaxis of AD.

CONCLUSION

This study suggests that a degree of presynaptic 5HT function in the subcortical 5HT projection region is compromised in AD patients even before the development of depression. Right DLPFC dysfunction in parallel with 5HT inactivation is also implicated in the progression of emotional and cognitive deterioration in AD.

ACKNOWLEDGMENTS

We thank Dr. Mitsuo Kaneko (Kaneko Clinic), Dr. Masanobu Sakamoto (Hamamatsu Medical Center), Toshihiko Kanno (Hamamatsu Medical Center), and Yutaka Naito (Japan Environment Research Corporation) for their clinical and technical support. This work was supported by a Research Grant for Longevity Science from the Ministry of Health, Labor, and Welfare, Japan.

REFERENCES

1. Lanctôt KL, Herrmann N, Mazzotta P. Role of serotonin in the behavioral and psychological symptoms of dementia. *J Neuropsychiatry Clin Neurosci.* 2001; 13:5–21.
2. Mann DM, Yates PO. Serotonin nerve cells in Alzheimer's disease [letter]. *J Neurol Neurosurg Psychiatry.* 1983;46:96.
3. Palmer AM, Francis PT, Benton JS, et al. Presynaptic serotonergic dysfunction in patients with Alzheimer's disease. *J Neurochem.* 1987;48:8–15.
4. Assal F, Alarcón M, Solomon EC, Masterman D, Geschwind DH, Cummings JL. Association of the serotonin transporter and receptor gene polymorphisms in neuropsychiatric symptoms in Alzheimer disease. *Arch Neurol.* 2004;61:1249–1253.
5. Curcio CA, Kemper T. Nucleus raphe dorsalis in dementia of the Alzheimer type: neurofibrillary changes and neuronal packing density. *J Neuropathol Exp Neurol.* 1984;43:359–368.
6. Zubenko GS, Moossy J, Martinez AJ, et al. Neuropathologic and neurochemical correlates of psychosis in primary dementia. *Arch Neurol.* 1991;48:619–624.
7. Nyth AL, Gottfries CG. The clinical efficacy of citalopram in treatment of emotional disturbances in dementia disorders: a Nordic multicentre study. *Br J Psychiatry.* 1990;157:894–901.
8. Petracca G, Tesón A, Chemerinski E, Leiguarda R, Starkstein SE. A double-blind placebo-controlled study of clomipramine in depressed patients with Alzheimer's disease. *J Neuropsychiatry Clin Neurosci.* 1996;8:270–275.
9. Kepe V, Barrio JR, Huang SC, et al. Serotonin 1A receptors in the living brain of Alzheimer's disease patients. *Proc Natl Acad Sci USA.* 2006;103:702–707.
10. Meltzer CC, Smith G, DeKosky ST, et al. Serotonin in aging, late-life depression, and Alzheimer's disease: the emerging role of functional imaging. *Neuropsychopharmacology.* 1998;18:407–430.
11. Truchot L, Costes N, Zimmer L, et al. A distinct [^{18}F]MPPF PET profile in amnestic mild cognitive impairment compared to mild Alzheimer's disease. *Neuroimage.* 2008;40:1251–1256.
12. Lavoie B, Parent A. Immunohistochemical study of the serotoninergic innervation of the basal ganglia in the squirrel monkey. *J Comp Neurol.* 1990;299:1–16.
13. Lavoie B, Parent A. Serotoninergic innervation of the thalamus in the primate: an immunohistochemical study. *J Comp Neurol.* 1991;312:1–18.
14. Thomas AJ, Hendriksen M, Piggott M, et al. A study of the serotonin transporter in the prefrontal cortex in late-life depression and Alzheimer's disease with and without depression. *Neuropathol Appl Neurobiol.* 2006;32:296–303.
15. Levy-Cooperman N, Burhan AM, Rafi-Tari S, et al. Frontal lobe hypoperfusion and depressive symptoms in Alzheimer disease. *J Psychiatry Neurosci.* 2008;33:218–226.
16. Davidson RJ, Pizzagalli D, Nitschke JB, Putnam K. Depression: perspectives from affective neuroscience. *Annu Rev Psychol.* 2002;53:545–574.
17. Mann UM, Mohr E, Chase TN. Rapidly progressive Alzheimer's disease [letter]. *Lancet.* 1989;2:799.
18. Ouchi Y, Nakayama T, Kanno T, Yoshikawa E, Shinke T, Torizuka T. In vivo presynaptic and postsynaptic striatal dopamine functions in idiopathic normal pressure hydrocephalus. *J Cereb Blood Flow Metab.* 2007;27:803–810.
19. Weintraub D, Xie S, Karlawish J, Siderowf A. Differences in depression symptoms in patients with Alzheimer's and Parkinson's diseases: evidence from the 15-item Geriatric Depression Scale (GDS-15). *Int J Geriatr Psychiatry.* 2007;22:1025–1030.
20. Ouchi Y, Yoshikawa E, Okada H, et al. Alterations in binding site density of dopamine transporter in the striatum, orbitofrontal cortex, and amygdala in early Parkinson's disease: compartment analysis for beta-CFT binding with positron emission tomography. *Ann Neurol.* 1999;45:601–610.
21. Sekine Y, Ouchi Y, Takei N, et al. Brain serotonin transporter density and aggression in abstinent methamphetamine abusers. *Arch Gen Psychiatry.* 2006;63:90–100.
22. Phelps ME, Huang SC, Hoffman EJ, Selin C, Sokoloff L, Kuhl DE. Tomographic measurement of local cerebral glucose metabolic rate in humans with (F-18)2-fluoro-2-deoxy-D-glucose: validation of method. *Ann Neurol.* 1979;6:371–388.
23. Palacios JM, Waeber C, Hoyer D, Mengod G. Distribution of serotonin receptors. *Ann N Y Acad Sci.* 1990;600:36–52.
24. Mai JK, Assheuer J, Paxinos G. *Atlas of the Human Brain.* San Diego, CA: Academic Press; 1997.
25. Logan J, Volkow ND, Fowler JS, et al. Effects of blood flow on [^{11}C]raclopride binding in the brain: model simulations and kinetic analysis of PET data. *J Cereb Blood Flow Metab.* 1994;14:995–1010.
26. Procter AW, Lowe SL, Palmer AM, et al. Topographical distribution of neurochemical changes in Alzheimer's disease. *J Neurol Sci.* 1988;84:125–140.
27. Ouchi Y, Yoshikawa E, Futatsubashi M, Okada H, Torizuka T, Kaneko M. Activation in the premotor cortex during mental calculation in patients with Alzheimer's disease: relevance of reduction in posterior cingulate metabolism. *Neuroimage.* 2004;22:155–163.
28. Yamamoto T, Hirano A. Nucleus raphe dorsalis in Alzheimer's disease: neurofibrillary tangles and loss of large neurons. *Ann Neurol.* 1985;17:573–577.

29. Hendricksen M, Thomas AJ, Ferrier IN, Ince P, O'Brien JT. Neuropathological study of the dorsal raphe nuclei in late-life depression and Alzheimer's disease with and without depression. *Am J Psychiatry.* 2004;161:1096–1102.
30. Ichimiya T, Suhara T, Sudo Y, et al. Serotonin transporter binding in patients with mood disorders: a PET study with [^{11}C](+)McN5652. *Biol Psychiatry.* 2002;51:715–722.
31. Li T, Holmes C, Sham PC, et al. Allelic functional variation of serotonin transporter expression is a susceptibility factor for late onset Alzheimer's disease. *Neuroreport.* 1997;8:683–686.
32. Aucoin JS, Jiang P, Aznavour N, et al. Selective cholinergic denervation, independent from oxidative stress, in a mouse model of Alzheimer's disease. *Neuroscience.* 2005;132:73–86.
33. Holthoff VA, Beuthien-Baumann B, Kalbe E, et al. Regional cerebral metabolism in early Alzheimer's disease with clinically significant apathy or depression. *Biol Psychiatry.* 2005;57:412–421.
34. Mayberg HS, Liotti M, Brannan SK, et al. Reciprocal limbic-cortical function and negative mood: converging PET findings in depression and normal sadness. *Am J Psychiatry.* 1999;156:675–682.
35. Kennedy SH, Evans KR, Krüger S, et al. Changes in regional brain glucose metabolism measured with positron emission tomography after paroxetine treatment of major depression. *Am J Psychiatry.* 2001;158:899–905.
36. Grafman J, Schwab K, Warden D, Pridgen A, Brown HR, Salazar AM. Frontal lobe injuries, violence, and aggression: a report of the Vietnam Head Injury Study. *Neurology.* 1996;46:1231–1238.
37. Eustache F, Piolino P, Giffard B, et al. 'In the course of time': a PET study of the cerebral substrates of autobiographical amnesia in Alzheimer's disease. *Brain.* 2004;127:1549–1560.
38. Mattson MP, Maudsley S, Martin B. BDNF and 5-HT: a dynamic duo in age-related neuronal plasticity and neurodegenerative disorders. *Trends Neurosci.* 2004;27:589–594.
39. Nelson RL, Guo Z, Halagappa VM, et al. Prophylactic treatment with paroxetine ameliorates behavioral deficits and retards the development of amyloid and tau pathologies in 3xTgAD mice. *Exp Neurol.* 2007;205:166–176.
40. Steele C, Rovner B, Chase GA, Folstein M. Psychiatric symptoms and nursing home placement of patients with Alzheimer's disease. *Am J Psychiatry.* 1990; 147:1049–1051.

Molecular and Functional Imaging for Drug Development and Elucidation of Disease Mechanisms Using Positron Emission Tomography (PET)

Manabu Tashiro[1], Toshihiko Fujimoto[2], Nobuyuki Okamura[4], Ren Iwata[3], Hiroshi Fukuda[5], and Kazuhiko Yanai[1,4]

Summary

Tohoku University has a more than 30-year-long history of molecular and functional imaging research using radiopharmaceuticals. This article provides a brief overview of various achievements in molecular and functional imaging at Tohoku University. It is noteworthy that many of these early studies were associated with positron emission tomography (PET) studies in oncology and neuroscience. Later, new application to sports sciences was initiated, and PET and [^{18}F]fluorodeoxyglucose ([^{18}F]FDG) has been used for exercise physiology and psychology studies. This technique, similar to the performance of autoradiography, allows subjects to be scanned just after carrying out exercise tasks. We have observed the metabolic effects of exercise on brain and skeletal muscles.

One of the important contributions we have made in neuroscience has been associated with the histaminergic neuronal system in the brain. The histaminergic system is associated with various autonomic functions such as the sleep-wake cycle and appetite control. Using PET and [^{11}C]doxepin, a ligand for histamine H1 receptors, various studies have been conducted regarding physiological changes such as those occurring in aging, and pathological changes such as those occurring in Alzheimer's disease (AD), depression, schizophrenia, and anorexia nervosa. In addition, PET and [^{11}C]doxepin has also been used for the evaluation of side effects due to histamine H1 receptor antagonists (antihistamines). Antihistamines are frequently used for the treatment of allergic disorders such as seasonal rhinitis, but these drugs can induce sedative side effects that can sometimes result in serious

[1]Division of Cyclotron Nuclear Medicine, Cyclotron and Radioisotope Center, Tohoku University, 6-3 Aoba, Aramaki, Aoba-ku, Sendai 980-8578, Japan
[2]Division of Radiopharmaceutical Chemistry, Cyclotron and Radioisotope Center, Tohoku University, 6-3 Aoba, Aramaki, Aoba-ku, Sendai 980-8578, Japan
[3]Center for the Advancement of Higher Education, Tohoku University, 41 Kawauchi, Aoba-ku, Sendai 980-8576, Japan
[4]Department of Pharmacology, Tohoku University Graduate School of Medicine, 2-1 Seiryo-machi, Aoba-ku, Sendai 980-8575, Japan
[5]Institute of Development, Aging and Cancer, Tohoku University, 4-1 Seiryo-machi, Aoba-ku, Sendai 980-8575, Japan

N. Tamaki, Y. Kuge (eds.)
Molecular Imaging for Integrated Medical Therapy and Drug Development.
DOI: 10.1007/978-4-431-98074-2_23, ©Springer 2010

traffic accidents. Objective measurement of the sedative property of antihistamines was established using histamine H1 receptor occupancy as a reliable index. Our additional functional imaging studies using [^{18}F]FDG and [^{15}O]H_2O have revealed the brain mechanisms of these sedative side effects in the brains of allergic patients.

Finally, we have been involved in the development of novel tracers for amyloid deposits in the brains of patients with AD and mild cognitive disorder. We have been conducting clinical studies of an ^{11}C-labelled tracer, [^{11}C]2-(2-[2-dimethyl-aminothiazol-5-yl]ethenyl)-6-(2-[fluoro]ethoxy)benzoxazole (BF-227). Our early evaluation has demonstrated that [^{11}C]BF-227 is a promising tracer for the differentiation of aged normal volunteers and AD patients. In future, PET will undoubtedly be used more frequently in drug development and for the early diagnosis of various diseases.

Key word [^{18}F]fluorodeoxyglucose (FDG) · sports medicine · [^{11}C]doxepin · histamine H1 receptor · [^{11}C]BF-227 · amyloid imaging

Introduction to Molecular and Functional Imaging

Molecular and functional imaging with nuclear medicine techniques has been useful to investigate endophenotypic alterations in a living human or animal body externally without perturbing biological phenomena. This nuclear medicine technique was founded in the early twentieth century, when a tracer technique was developed by Dr. George von Hevesy, a Nobel laureate in chemistry, in 1943. This technique was later applied to scintigraphy for human subjects, and was fused with computed tomography technology, positron emission tomography (PET), and single photon emission computed tomography (SPECT) established in the late twentieth century. Now this field, established as nuclear medicine, has been actively used for molecular and functional imaging.

Using PET as a tool for molecular and functional imaging, we can measure cerebral energy (glucose) consumption by injecting [^{18}F]fluorodeoxyglucose ([^{18}F]FDG). Increased regional brain activity may result in increased demands for glucose and oxygen, inducing dilation of brain capillaries. This can be accompanied by an increase in regional cerebral perfusion, which can be measured using PET and radiolabeled water ([^{15}O]H_2O), and other methods such as functional magnetic resonance imaging (fMRI) and near-infrared spectroscopy (NIRS). Nowadays, PET is more often used for measuring regional brain glucose consumption and for evaluating neurotransmission function. In the human brain, neurotransmitters can exert their actions even in very small amounts. It is not easy to visualize the actions of neurotransmitters in the living human brain externally without using a highly sensitive technique such as PET. In addition, PET enables the quantification of interactions between neurotransmitters and neuroreceptors. PET has been used for more than 30 years as a tool for molecular and functional imaging at Tohoku University.

Research and Education in Molecular and Functional Imaging at Tohoku University

In 1977, the Cyclotron and Radioisotope Center (CYRIC) was founded at Tohoku University for the multipurpose use of a cyclotron, including nuclear physics, nuclear chemistry, solid-state physics, and radioisotope production for biology and medicine. Clinical studies were started at CYRIC in 1982 following the first installation of a PET scanner in 1981. In 1976, the production of [^{18}F]FDG had already been successfully done, initially for brain research at CYRIC, and the use of [^{18}F]FDG was later applied to oncology research. The challenge of using [^{18}F]FDG for cancer imaging was based on Matsuzawa's concept of "fishing for cancer with baits." He claimed that "cancer cells were always hungry and almost blind, therefore they try to eat anything including false sugars, amino acids, and nucleic acids." Soon, Fukuda and colleagues reported the applicability of [^{18}F]FDG PET for diagnosing metastatic liver cancer, in 1982 [1]. Later, in 1983, [^{11}C]methionine was proven to be useful for lung cancer detection [2]. In addition, [^{18}F]fluorodeoxygalactose was also demonstrated to be useful for cancer imaging, in 1986 [3] (Fig. 1). The first international symposium on PET oncology was held in 1985, and soon after PET oncology became known worldwide. Recently, a new tracer for oncology imaging, [^{18}F]O-fluoro-methyl-tyrosine (FMT), has been examined for its

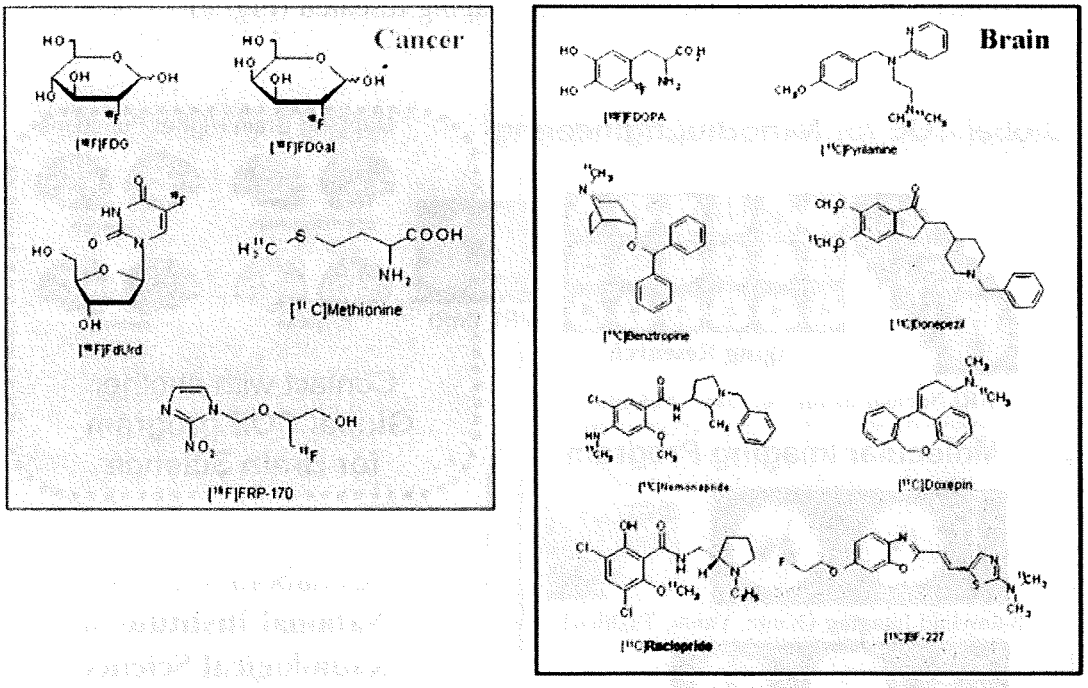

Fig. 1. Examples of radiotracers that have been used at Tohoku University. *[^{18}F]FDGal*, [^{18}F] fluorodeoxygalactose; *[^{18}F]Fd Urd*, [^{18}F] fluorodeoxyuridine; *[^{18}F]FDG*, [^{18}F]fluorodeoxyglucose; *[^{18}F]FRP*, 1-(2-fluoro-1-[hydroxymethyl]ethoxy) methyl-2-nitroimidazole; *[^{11}C]BF-227*, [^{11}C]2-(2-[2-dimethylaminothiazol-5-yl]ethenyl)-6-(2-[fluoro]ethoxy)benzoxazole. Tohoku University has carried out human positron emission tomography (PET) studies for more than 25 years, since 1982

usefulness for oncology diagnosis [4]. [^{18}F]1-(2-fluoro-1-[hydroxymethyl]ethoxy) methyl-2-nitroimidazole ([^{18}F]FRP-170) has been synthesized for imaging hypoxic cells resistant to radiation therapy; this tracer has been applied to cancer patients to determine its usefulness for diagnosing hypoxic malignant cells that tend to be resistant to radiation therapy [5].

For brain research, we have mainly used [^{18}F]fluoro-L-DOPA (dopamine metabolism) [6, 7], [^{11}C]YM9151–2 and [^{11}C]nemonapride (dopamine D2 receptors) [6, 8], [^{11}C]benztropine (muscarinic acetylcholine receptors) [9], and [^{11}C]doxepin (histamine H1 receptors; H1R) [10] for human brain studies. Brain activation studies during running [11] and car-driving [12] have also been initiated. Various new tracers have been introduced, such as [^{11}C]BF-227, for imaging beta-amyloid deposition [13], and [^{11}C]donepezil, for evaluating the function of acetylcholinergic nerves [14]. [^{11}C]BF-227 has recently attracted the attention of many Japanese investigators as the first domestic probe for the clinical examination of AD patients. [^{11}C]donepezil has also been used previously in clinical examinations at Tohoku University [14] (Fig. 1).

Since 2006, Tohoku University has managed the "Molecular Imaging Program," including an educational course for postgraduate students. This program has been organized in collaboration with the National Institute of Radiological Science (Chiba, Japan). In this program, CYRIC has been playing important roles in performing experiments and in further education. Below, we outline our recent achievements in molecular and functional imaging research (Fig. 2).

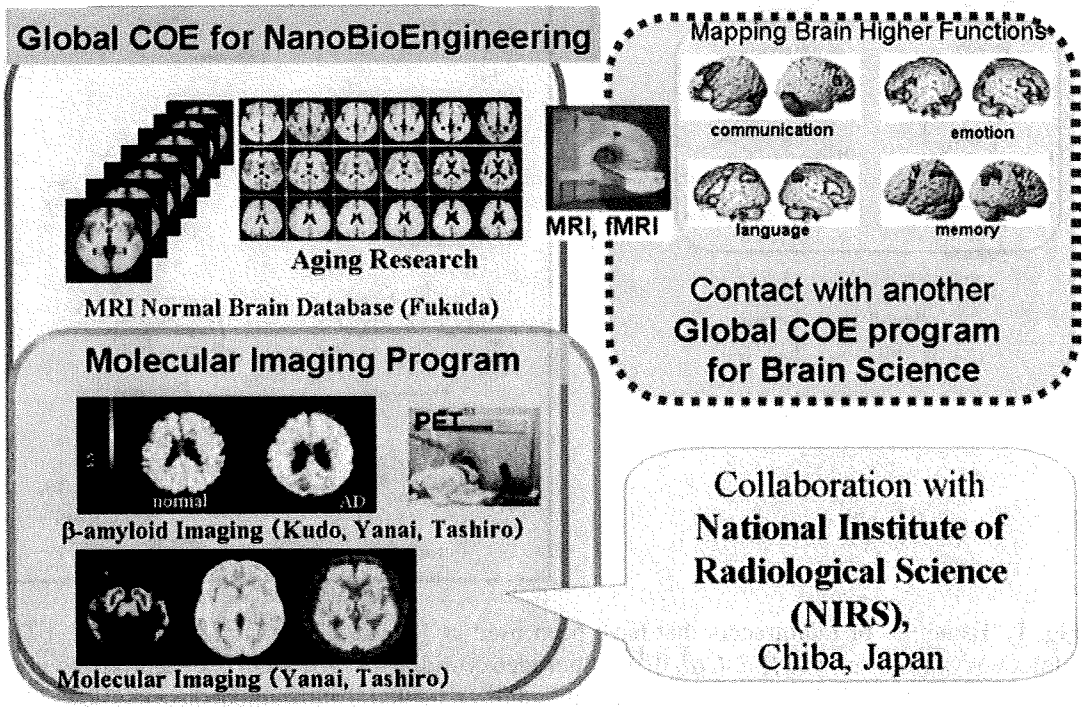

Fig. 2. Organizations and projects of Tohoku University's current work in molecular and functional imaging and brain research. *COE*,; *MRI*, magnetic resonance imaging; *fMRI*, functional magnetic resonance imaging; *AD*, Alzheimer's disease; *SUV*, standardized uptake value

Exercise and Brain Imaging Related to Physical and Mental Health

In the scope of applying PET to health promotion science, we have performed imaging studies in subjects during various forms of exercise such as running and bicycle riding. We have scanned not only the brain [11, 15] but also the skeletal [15, 16] and cardiac muscles [17]. By conducting whole-body scanning, we can obtain a whole-body map of energy metabolism in the living human body [16] (Fig. 3). Regional cerebral metabolic changes induced by exercise have been examined in animals with an autoradiography technique using [^{14}C]deoxyglucose ([^{14}C]2-DG) as a tracer, because it did not require the simultaneous scanning of subjects during exercise [18, 19]. These studies provided the first functional indices of brain activity with respect to exercise. Using this technique, Sharp [20] demonstrated a regional increase in glucose uptake in the cerebellar vermis of swimming rats. Human studies were later conducted by Herholz and coworkers [21] in the late 1980s, first using a ^{133}Xe clearance method for studying regional changes in brain activity. Later, Fink and coworkers [22] demonstrated regional activation during and immediately after an ergometer task by PET using [^{15}O]H_2O. In addition, Mishina and coworkers [23] applied [^{18}F]FDG PET to the neuropathological evalu-

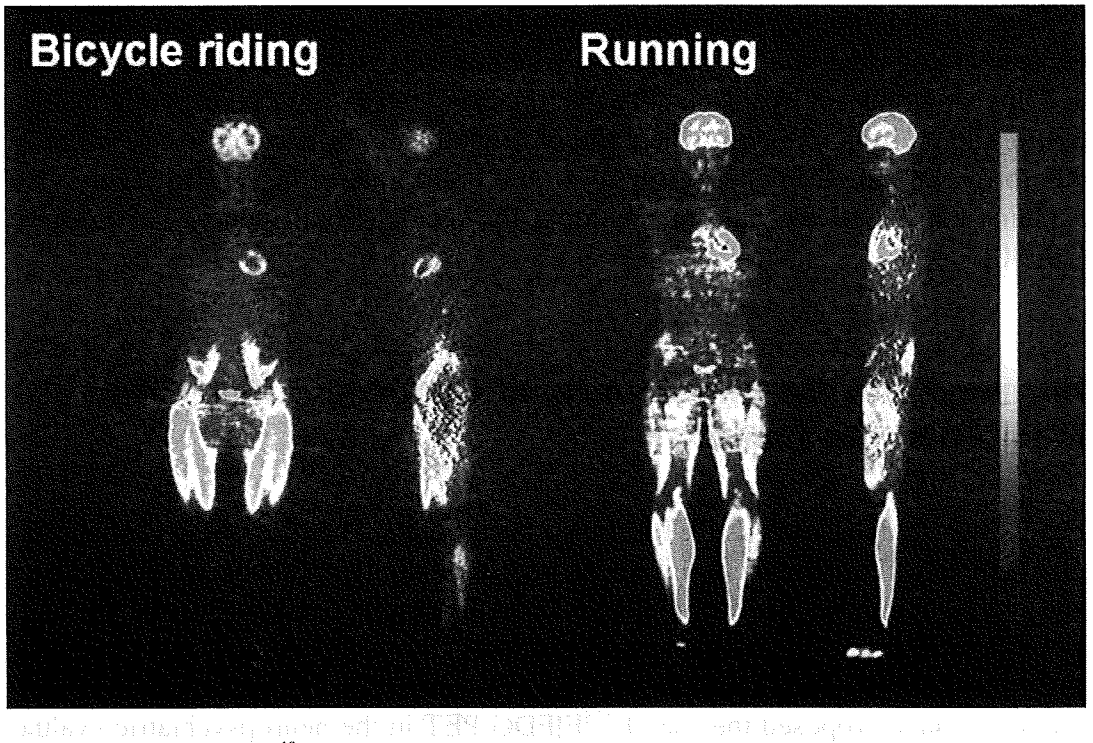

Fig. 3. An example of [^{18}F]FDG PET use in exercise physiology. A clear difference can be seen between bicycle riding (*left*) and running (*right*).

ation of patients with olivo-pontine-cerebellar atrophy manifesting gait disturbances; these patients exhibited a decreased response to a walking task in the cerebellar vermis compared with normal subjects.

We first applied [^{18}F]FDG PET to healthy human subjects undertaking a running task in the upright posture (Fig. 3). We demonstrated a relative increase in glucose uptake in the temporo-parietal association cortex, occipital cortex, premotor cortex, primary sensorimotor cortex, and the cerebellar vermis [24]. This was probably due to the higher energy consumption necessary for integrating multimodal sensory inputs. A relative reduction in glucose uptake was detected in the prefrontal cortex, temporal cortex, cerebellar hemisphere, brain stem, and striatum. The mean value of global brain glucose uptake was relatively lower in the runners than in resting controls [24]. Kemppainen and coworkers [25] later demonstrated a significant reduction of the regional glucose metabolic rate in all cortical regions in correlation with exercise intensity. They also pointed out that exercise could be associated with adaptive metabolic changes in the frontal cortex [25]. Thus, global and regional brain metabolic decline, especially in the limbic and frontal regions, was observed using [^{18}F]FDG PET [24, 25]. It is easy to explain the metabolic increase in the regions directly associated with the execution of exercise tasks, while it is not so easy to explain the mechanism of the relative decrease in the regions not involved in exercise. Previous imaging studies in patients with anxiety disorders demonstrated increased glucose metabolism in the limbic and frontal regions [26, 27]. We speculated that the metabolic reduction in the frontal and limbic regions in runners was associated with emotional changes, including the phenomenon called "runner's high" [28].

Dietrich and Sparling [29] reported that endurance exercise impaired prefrontal-dependent cognitive ability in healthy volunteers. Dietrich [30] later proposed a new theory (transient hypofrontality theory; THT) to explain the metabolic reduction in the prefrontal region, where the prefrontal activity is suppressed indirectly due to the limitation in energy supply to the brain. Interestingly, this theory also explains the neural mechanism regarding the mental health benefits of exercise [29, 30].

Imaging Study for Improvement of Quality of Life (QOL) in Patients with Cancer

Functional imaging such as PET has also been used for studies of psychiatric disorders in patients with physical diseases such as malignant tumors. Because cancer and cancer treatments have various effects on the central nervous system, the diagnosis of psychiatric symptoms in cancer patients is, in part, problematic. Molecular and functional imaging could be used as a supplementary diagnostic tool. Previously, we have proposed the use of [^{18}F]FDG PET in the neuropsychiatric evaluation of cancer patients, and we have performed a series of studies to examine whether or not the images of a cancer patient's brain are normal. It is now widely

accepted that psychological factors are as important as external factors in disease progression. Thus, psychological evaluation and patient care are very important, not only for improving quality of life (QOL) but also for prolonging survival. If we assume that a certain psychological disturbance truly exists in a patient, to the extent of affecting systemic function, it is also possible for their brain activity to have significant alterations. Thus, it seems reasonable to think that cancer patients may manifest a corresponding abnormality in their functional brain images. Our preliminary work has demonstrated regional hypometabolic findings, mainly in the prefrontal cortex, limbic structures, and striatum, in Japanese cancer patients [31, 32]. Common findings in these studies were hypometabolism in the prefrontal cortex, anterior and posterior cingulate, insular cortex, and striatum. These regions were similar to those demonstrated in previous neuroimaging studies of patients with major depression showing commonly repeated findings of hypometabolism in the prefrontal cortex, anterior cingulate gyrus, and basal ganglia. Our additional cross-sectional study in Japanese cancer patients showed that the depth of hypometabolic findings tended to fluctuate in some regions and constantly decreased in other regions [33]. Finally, we demonstrated that regional hypometabolism in the prefrontal cortex was negatively correlated with the subjective measure of depression in cancer patients. Nowadays, mild cognitive impairment after chemotherapy, so-called chemo-fog, has been studied intensively in association with QOL [34].

Molecular and Functional Imaging of the Histaminergic Nervous System

Psychosocial stress has been associated with increased rates of various psychiatric disorders, such as major depression, schizophrenia, anxiety, and eating disorders in our daily lives. The incidence of cognitive disorders is also increasing. We have recently conducted a variety of studies to elucidate the pathophysiological mechanisms of psychiatric disorders mentioned above [35–39], putting emphasis on alterations in neural transmission in the histaminergic neuronal system [35]. For this purpose, [^{11}C]doxepin is the tracer of choice for imaging histamine H1 receptors (H1Rs). Using PET and [^{11}C]doxepin, a large amount of evidence has been accumulated regarding the role of the histaminergic neuronal system in the pathophysiology of these disorders. In our recent studies, histamine H1 receptor binding was measured, by PET and [^{11}C]doxepin, in 10 normal male subjects and 10 patients with schizophrenia [36], 10 patients with major depression [37], and 10 patients with AD [39], respectively, as well as in 10 normal female subjects and 12 female patients with anorexia nervosa [38]. In these studies, significant reductions in H1 receptor binding were observed in the patients with schizophrenia, major depression, and AD, while a significant increase was observed in the patients with anorexia nervosa [35–39].

In addition, PET and [^{11}C]doxepin is also useful for the evaluation of drug-induced side effects and the elucidation of their mechanism [35]. Some of the most frequently used therapeutic drugs for allergies such as seasonal pollinosis, or hay fever, are H1R antagonists (antihistamines). There are many available antihistamines, but some of them have sedative side effects. Therefore, it is important to develop an objective and reliable method for measuring the strength of such sedative side effects [35, 40, 41]. To date, we have studied the mechanism of functional suppression in signal transmission through H1Rs in the brain. Usually, antihistamines are used to suppress the actions of mast cells in the peripheral blood and to control allergic reactions. However, some of these drugs may enter the brain and suppress the signal transmission of intracerebral H1Rs. As a result, it becomes difficult to maintain arousal (sedative effects), and sometimes these drugs may cause us to make mistakes during work or while driving, resulting in decreased work efficiency or traffic accidents. Considering such a background, the objective measurement of the sedative effects of these drugs becomes very important.

We have succeeded in quantifying the strength of the sedative effects of antihistamines in terms of H1R occupancy (rate) in the brain using PET, and we have measured this clinically. Previously, to evaluate drug sedative effects, investigators have used macroscopic behavioral techniques such as the measurement of psychomotor performance, including psychomotor speed and accuracy, as well as the measurement of subjective sleepiness, using many volunteer subjects [35, 40]. Recently, we conducted a clinical test to evaluate the sedative profile of bepotastine besilate, a new antihistamine developed in Japan [40]. The basic pharmaceutical classification of this antihistamine has been "a mildly sedative antihistamine". We succeeded in obtaining supporting data regarding this classification using PET [35] (Fig. 4).

From the viewpoint of cognitive neuroscience, the category of cognitive function (psychomotor performance) measured in antihistamine studies is mainly "vigilance and attention." The sedative side effects of antihistamines have been recognized to be potentially dangerous in our daily tasks such as car driving, but the mechanism underlying these effects has not yet been elucidated well. We, therefore, attempted to elucidate the brain mechanism of impaired performance by using a car-driving simulator and [^{15}O]H_2O PET [42]. We examined regional cerebral blood flow (rCBF) responses during a simulated car-driving task following the oral administration of D-chlorpheniramine, using [^{15}O]H_2O PET. The results of the performance evaluation revealed that part of the driving performance (lane deviation) significantly increased in the D-chlorpheniramine condition compared with the placebo condition, while subjective sleepiness was not significantly different between the two drug conditions. In addition, brain imaging analysis suggested that D-chlorpheniramine tended to suppress the regional brain activities associated with visuo-spatial cognition and visuo-motor coordination [42].

Thus, nuclear medicine techniques are very useful for the objective evaluation of the intensities and mechanisms of the effects of various drugs on the brain. These data can be used for the development of new drugs with reduced side effects.